

Corrosion Performance of Ta/Ni Ions Implanted with WO₃/FTO

S. Hoseinzadeh^{a*} and A. H. Ramezani^b

Keywords : Corrosion, Nano composite; Ion implantation; TaN; AFM

ABSTRACT

In the last decades an extensive number of research papers published on Nano chip electrode and cathode electrochromic materials. The surface bombardment with inert gases mainly procreate structural modifications, developing topography and morphology that atomic force microscopy (AFM) analysis reveals significant differences on the surface. In this article, the efficacy of Tantalum (Ta), Nitrogen (Ni), and Tungsten Tri Oxide (WO₃) ion implantation on surface structure is perused. The ions' implantation manner was operated at 30 keV with various doses. The electrical resistance to tantalum corrosion is investigated. The surface topography and nanostructures property were investigated on nanocomposite by looking at current-voltage curves. In addition to TaN, WO₃ powders deposited on fluorine-doped tin oxide (FTO)-coated glass with using the physical vapor deposition (PVD) apparatus are determined as an Electrochromic devices (ECD). Following The change of surface morphology, roughness, corrosion resistance is evaluated by using the (AFM) and Energy Dispersive X-Ray (EDX) analysis plus, the elemental composition is characterized by energy-dispersive X-ray (XRD) and electrical resistance analysis. Consequently, Ta-Ni-n type WO₃ with more trap centers (rough surface) can be suggested as a future of ECD and Nano devices.

Paper Received January, 2018. Revised July, 2018. Accepted August, 2018. Author for Correspondence: S. Hoseinzadeh.

^a *Young Researchers and Elite Club, West Tehran Branch, Islamic Azad University, Tehran, Iran.*

^b *Department of Physics, West Tehran Branch, Islamic Azad University, Tehran, Iran*

*Corresponding author. E-mail address:
Hoseinzadeh.siamak@gmail.com

INTRODUCTION

Ion implantation has ordinarily been applied as a surface modification technique to advance surface properties. High dose ion implantation is a process to modify the mechanical properties of metals. One of the most important metals which used in biocompatibility is tantalum (Ta) due to improved performance and high corrosion resistance of tantalum after performing implantation. For many years, tantalum is used widely in experimental works (Hoseinzadeh, S. et al., 2018). This is because of its properties. Excellent biocompatibility, low density, high corrosion resistance and suitable mechanical properties cause to use it in various studies. Recently, tantalum thin films used frequently in industry due to some characteristics like highly corrosion-resistant, chemical inertness and high melting point (Hübler, R. 1999). Because of the size and weight advantages, tantalum capacitors are attractive for portable telephones, personal computers, automotive electronics, Smart Windows, electrochromic devices (ECD) and Cameras. There are many reports about effects of tantalum for industrially exposed workers. Therefore many researches focused to improve its characteristics. Among them, ion implantation is used frequently (Ramezani, A.H. et al., 2017). On the other hand, the cathode deposited on fluorine-doped tin oxide (FTO) coated glass substrate by PVD (Physical vapor deposition) method, needs more trap centers as well as a cathode for electrochromic devices (ECD) and Nano devices that were investigated with (Bahari, A. et al., 2018; Hoseinzadeh, S. et al., 2017 Najafi-Ashtiani, H., 2016).

Nano electronic materials and devices have attracted lots of attention among the Nano-engineering community in recent years. Nano electronic devices are essential parts for designing in advanced technologies, 3D printing (Zolfagharian, A. et al., 2018, Zolfagharian, A. et al., 2018; Zolfagharian, A. et al., 2018), MEMS and harvesting energy (Derakhshani, M. et al., 2018; Derakhshani, M. et al. 2018; Hashemi, H. S., 2013), electronic and magnetic devices (Li, K. et al., 2017; Som, D. et al., 2017). The fundamental element of Nano electronic devices can have mechanical, electronic or chemical significance; so, studying the characteristic behavior of these devices along with characterization of their

intrinsic elements become an interesting topic for researchers. A lot of previous works examined the mechanical operation-based nanomaterials, which has application in Nano electronic devices. Ghasemi et al. characterized the mechanical behavior of carbon nanotubes considered as nanobeams with different clamping and geometries (Ghasemi, A. et al. 2012; Ghasemi, A. et al., 2015). Materials such as polymers (Tehrani, M. et al. 2018; Tehrani, M. et al., 2017; Wu, C. et al.; 2018, Alvavaz, A. et al. 2017), graphene-oxide (Benedetti, I. et al., 2018) and polymer-graphene composites (Safaei, B. et al., 2018), SiC, Al₂O₃ and copper nanoparticles (Hoseinzadeh, S. et al., 2017; Ghasemiasl, et al., 2018) are studied in the works as mentioned earlier which have application as a mechanical element in some Nano electronics devices. However, there is another category of Nano electronic devices, which operate based on the chemical characteristic and behavior of nanomaterials. Moreover, Tantalum/Nitrogen has many attractive characteristics, for instance, high melting point, hardness, chemical stability and thermal conductivity and low electrical resistivity, which make it possible to use as diffusion barriers for proper cabling classifications in silicon-based integrated circuits (IC) (Ramezani, A.H. et al., 2016).

Here in this study, we focus on this kind of materials. Corrosion reactions in aqueous media are oxidation-reduction reactions in which the free energy change determines the utility of the reaction and electrode kinetics controlled yonder. The change of surface morphology, roughness, corrosion resistance is evaluated by using the (AFM) analysis and the structure phases of and WO₃ have analyzed with X-ray diffraction (XRD) technique. The obtained results indicate that TaN with more trap centers can be identified as a possible element of the subsequent ECD and Nano devices.

MATERIAL AND EXPERIMENT

Ion bombardment is carried out on Tantalum samples with a size of 1cm×1cm and 1 mm thicknesses by the ion implantation facility which implemented in Plasma Physics Research Center (PPRC). Figure 1 shows the schematic of ion implantation system. Ion bombardment procedure is performed by Nitrogen ions (99.999%) with the energy of 30 keV and doses of 5×10^{17} ion/cm² at the ambient temperature, and the angle is 90° between the implanted ions and surface of samples. Ere ion implantation, sample surfaces were polished to a glossy coating by diamond paste and then cleaned ultrasonically in Alcohol and acetone bath. The extracted ions (Without mass selection) are accelerated to the maximum energy of 30 keV.

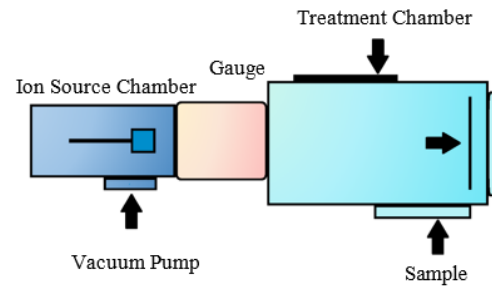


Fig. 1. Diagram and design of ion implantation system

The samples are implanted at applications of 5×10^{17} ions/cm². The ion beam cross section is expected to cover all the sample area uniformly. A thermocouple is used to measure the samples temperature during the implantation. The implantation parameters are listed in Table 1. Before starting ion implantation, the entire sample had room temperature. This temperature changed through implantation because of heat transfer from ion bombardment to the representations.

Table 1. The process parameter during implantation

Sample (#)	Energy (keV)	Ion current ($\mu\text{A}/\text{cm}^2$)	Dose (ions/cm ²)	Temp. (°c)
Un-implanted	-	-	-	-
Sample implanted	30	40	3×10^{17}	100

For constructing FTO/TaN/WO₃ electrochromic arrangement is deposited toward fluorine-doped tin oxide (FTO) coated glass substrate by physical vapor deposition (PVD) method. Current (Å), deposition time (second) and deposition rate (Å/Sec) of PVD is shown in Fig. 2. In this method, first the WO₃ nanoparticles powder with an average rate of 0.4 \AA s^{-1} are deposited in vacuum on FTO substrate for 80 minutes. The maximum of current was about 3.5 mA in oxidation state for this sample. This arrangement (FTO/TaN/WO₃) can be used in ECDs with its excellent properties.

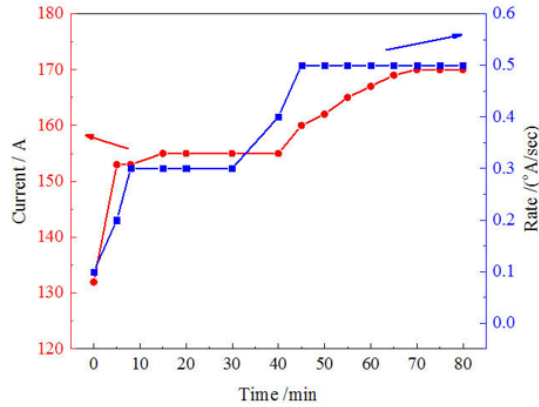


Fig. 2. The curves of current and deposition rate versus time in the deposition process

MASURMENTS AND RESULTS

There are various methods to study the structural properties and composition of the Tantalum samples. In present work, the microstructure of the samples before and after ion implantation is characterized by X-ray diffraction (XRD) analysis using STOE model STADI MP system using Cu α radiation (wavelength = 1.5405 Å) with a tungsten filament at 40 kV, 40 mA and step size of 0.04. The implantation-induced modification of surface roughness is studied employing an atomic force microscopy (AFM). The facility was an AFM (SPM Auto Probe CP, Park Scientific Instruments, and USA) in contact mode with low stress. In the following the measurements are described in details.

X-ray diffraction (XRD) characterization

Fig. 2, shows the XRD patterns of un-implanted and implanted samples with nitrogen ions at different dose of $1 \times 10^{17} - 10 \times 10^{17}$ ions/cm² and energy 30 Kev. In all XRD patterns, in addition to four peaks at $2\theta=38.66$, $2\theta=55.76$, and $2\theta=69.82$, $2\theta= 82.50$ degree which were related to the tantalum substrates, peaks of Ta (110), Ta (200), Ta (211) and Ta (200), respectively. Although at the implantation dose of 1×10^{17} ions/cm² new phases cannot be observed, but significant shifts of Ta lines toward lower 2θ angles are seen. This shift is also observed at higher implantation doses. Moreover, the amount of this shift is increased by the dose growth (e.g. see Fig 3). It is suggested that the nitrogen atoms are introduced into the spaces between the lattice positions and increase the distance between atomic layers. By increasing the ion dose in 3×10^{17} ions/cm² formation of hexagonal TaN_{0.43} is confirmed by XRD analysis (PDF cards #71-0265). The results show that by increasing the ion dose the peaks of both tantalum and tantalum nitride are shifted toward lower angles. The result showed that the intensity of TaN_{0.43} (111) is increased by nitrogen ion flux up to the dose of 1×10^{18} ions/cm². It can be concluded that by the ion

dose growth, more interstitial spaces in the target crystal are occupied by nitrogen atoms.

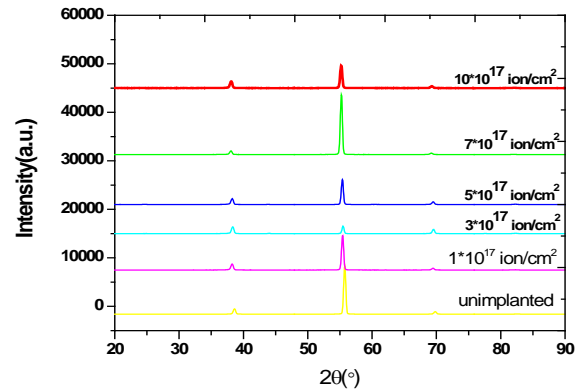


Fig. 3. XRD patterns of tantalum and implanted samples with nitrogen ion.

Atomic Force Microscopy (AFM) characterization

The surface roughness of the samples will undergo a substantial revision after bombardment. Atomic force microscopy (AFM) is manipulated in the probe of this characteristic. As seen in table 2 and figure 4 shows the fluctuation in average and root mean square roughness on tantalum. The surface roughness of tantalum increased up to 5×10^{17} ions/cm² dose. According to these images, by implantation dose, the topography and the size of grains on the samples change.

Table 2. Roughness measurement Ni ion implanted

Sample #	Un-implanted	Nitrogen implant
RMS roughness (Å)	12.5	21.3
Average roughness (Å)	8.78	17.35
Mean height (Å)	85.5	55.6

Root Mean Square (RMS) a kind of average sometimes used in statistics and engineering, often abbreviated as RMS. (Eq. 1-3). The surface root-mean-squared roughness in nm² (S_a), Mean in nm (S_m), two orientation roughness values (S_y, S_z) which show y-z (the Peak-Valley Height) plane are also measured and Root Mean Square (S_q). We take the surface roughness from the device and do not calculate ourselves, but the calculator performs the formula (Dastan, D. et al., 2016):

$$S_a = \frac{1}{N} \sum_{l=0}^{N-1} |z(x_l)| \quad (1)$$

$$S_m = \frac{1}{N} \sum_{l=0}^{N-1} z(x_l) \quad (2)$$

$$S_q = \sqrt{\frac{1}{N} \sum_{l=0}^{N-1} (z(x_l))^2} \quad (3)$$

Data on the Root Mean Square (RMS) roughness, half-value roughness and medium altitude which was collected from the AFM results are reported in Table 2. It ministers that when ion implantation is started, the RMS roughness increased, while it decreased at the final dose. It also appears that the manner of surface diffusion caused by ion bombardment contracts roughness. There was a significant change in areas such as roughness, grain size, its distribution for the un-implanted sample, and examples implanted with nitrogen ions.

It can be obviously seen that the sample surface roughness undergoes a substantial change after bombardment. In the case of un-implanted (Fig.4) there is a smooth surface whose surface morphology contained many small hillocks, and the root mean-square roughness of the surface has been further estimated. The implantation-induced modification of surface roughness and surface topography of WO_3 were studied employing atomic force microscopy (Fig. 5). The facility was an AFM in contact mode with a low-stress Tantalum nitride tip of less than 20 nm radiuses and a tip opening of 18 (Najafi-Ashtiani, H., 2018).

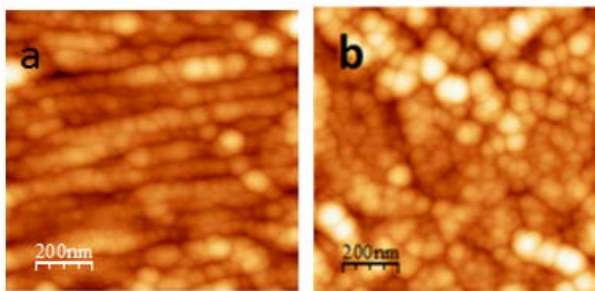


Fig. 4. AFM images of sample surfaces Un-implanted (a) and Implanted with Nitrogen (b)

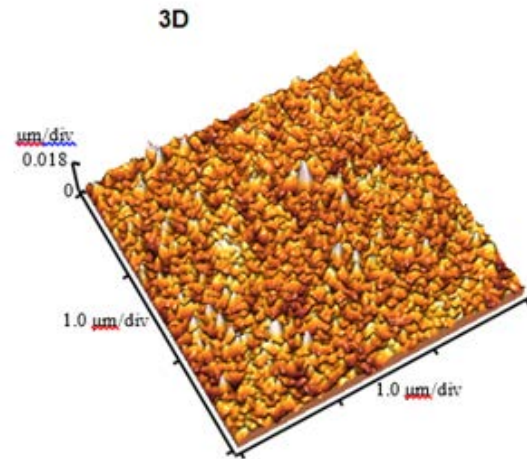
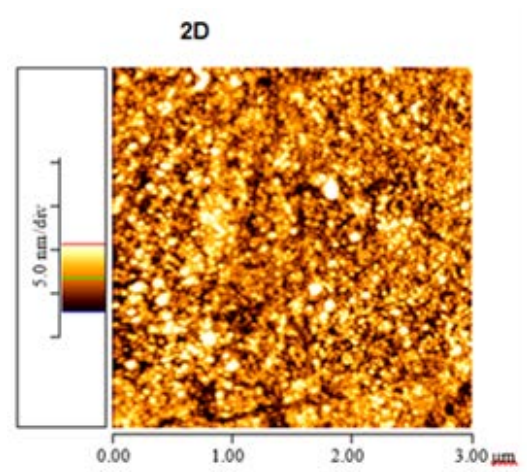


Fig. 5. 2D-3D AFM images of WO_3

As stated before, AFM is used for the investigation of surface topography and roughness of Ta/N and WO_3 sample surface as an example is described with DMSPM software image and data measurement that is shown in Fig. 6.

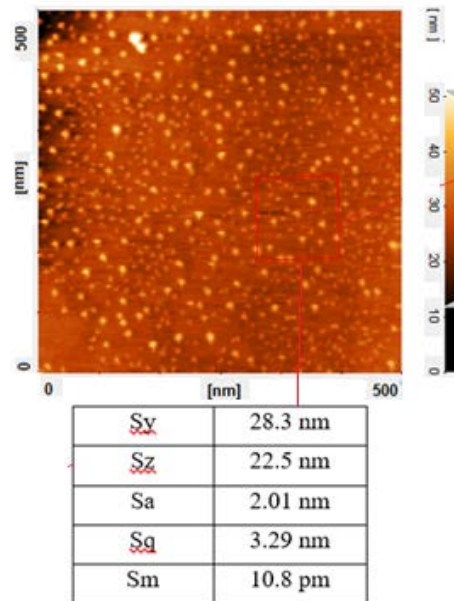


Fig. 6. The surface roughness of WO_3 measured with DM-SPM software

As fig. 7 shown, the ion dose increases, the surface morphology has a significant change and a notable growth in the surface roughness appear. For lowest implantation dose (i.e. 1×10^{17} ions/cm²), the roughness, grain size and its distribution of samples have no substantial change. But the average grain size (AGS) and sample's roughness are changed for the next doses.

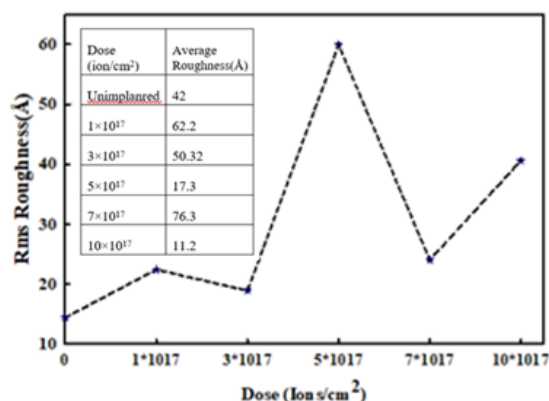


Fig. 7. Average and Rms surface roughness of unimplanted and nitrogen ion implanted Ta

Energy Dispersive X-Ray (EDX) analysis

One of the parameters which are investigated in this work is the friction coefficient. To show the friction of samples which are produced by ion implantation, Energy Dispersive X-Ray (EDX) images are analyzed. According to Table 3, the low concentration of retained nitrogen atoms is in agreement with the XRD result where no nitride phase was confirmed.

Table 3. Composition of the different Ta-N (Method EDX)

Sample (#)	Dose Ions/cm ²	Ta (%)	N (%)	N/Ta Ratio
1	1×10 ¹⁷	66.39	4.68	0.07
2	3×10 ¹⁷	69.46	13.82	0.19
3	5×10 ¹⁷	66.75	14.33	0.21
4	7×10 ¹⁷	65.13	13.31	0.20
5	10×10 ¹⁷	67.22	12.16	0.18

Electrical resistivity

Figure 7 shows the linear I-V curves obtained for samples. Also, it shows the results of electrical resistivity modifications at room temperature. As it shows there is an improvement in the electrical resistivity of the sample's surface with a growing dose. According to results, a robust relationship between the resistivity and the RMS roughness can be perceived. On the other hand, the resistivity values for the tantalum acquired using ion implantation technique have been in a range of 178-287 mΩ.cm. It can be seen that the electrical resistivity for the tantalum which doses 1×10¹⁸ ion/cm², had a high value of 287 mΩcm. Similar behavior of the sheet resistance of 38 keV nitrogen implanted tantalum film on glass for doses ranging from 3 ×10¹⁷ to 10 × 10¹⁷ ions/cm² has been reported elsewhere [4].

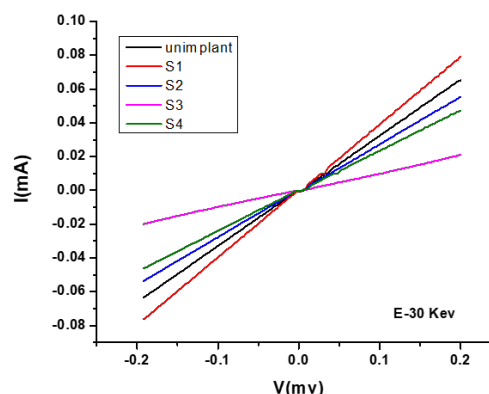


Fig. 9. I-V curves of current

CONCLUSION

Using the XRD patterns and AFM analysis the effect of nitrogen ion implantation on surface structure is investigated. Based on experimental results, increasing the ion dose cause to significant changes in the surface morphology and more interstitial spaces in the target crystal are occupied by nitrogen atoms. This increasing leads to significant growth in the surface roughness. Also, among the different values such as surface roughness, grain size, and ion concentration of the nitrogen, grain size has the strongest effect on hardness. The parameter which depends on surface roughness and hardness is friction coefficient. This parameter decreases in implanted samples in comparison with that of the tantalum samples. The EDX analysis show that the factors which are effective in improving wear resistance are friction and roughness, because of the reduction the friction coefficient the transfer tangent power in the samples surfaces decreased. Also, with increasing the nitrogen dose, corrosion rate decreases. And pitting local corrosion is observed on the surfaces of the samples evidently.

Furthermore enhancing nitrogen flux increased surface roughness and average resistance of samples. The electrical resistivity of tantalum of implanted samples especially after increasing ion dose increased. This cathode with more trap centers and possible surface dangling bonds can be advised for the future of ECD and Nano electronic devices.

REFERENCES

- Ramezani, A.H., Hoseinzadeh, S. & Bahari, A. J Inorg Organomet Polym (2018) 28: 847. <https://doi.org/10.1007/s10904-017-0769-4>
- Hübler, R. Surface and Coatings Technology 1999; 116-119: 1111-1115
- G.S. Chen, S.T. Chen: J. Appl. Phys. 87, 8473 (2000)
- A. H. Ramezani, A. H. Sai, and A. Shokouhy, Int

- Nano Lett 7 51-57 (2017)
- Hoseinzadeh, S., Ghasemiasl, R., Bahari, A. et al. *J Mater Sci: Mater Electron* (2017) 28: 14446. <https://doi.org/10.1007/s10854-017-7306-7>
- Hoseinzadeh, S., Ghasemiasl, R., Bahari, A. et al. *J Mater Sci: Mater Electron* (2017) 28: 14855. <https://doi.org/10.1007/s10854-017-7357-9>
- Hoseinzadeh, S., Ghasemiasl, R., Bahari, A. et al. *Journal of Elec Materi* (2018) 47: 3552. <https://doi.org/10.1007/s11664-018-6199-4>
- Hamed Najafi-Ashtiani, Ali Bahari, Shahram Ghasemi, A dual electrochromic film based on nanocomposite of aniline and o-toluidine copolymer with tungsten oxide nanoparticles, *Organic Electronics*, Volume 37, 2016, Pages 213-221
- Zolfagharian, A., Kaynak, A., Khoo, S.Y., Kouzani, A.Z., "Polyelectrolyte Soft Actuators: 3D Printed Chitosan and Cast Gelatin", *3D Print. Addit. Manuf.* 5 (2), 138-150, 2018
- Zolfagharian, A., Kouzani, A.Z., Khoo, S.Y., Noshadi, A., Kaynak, A., "3D printed soft parallel actuator", *Smart Mater. Struct.*, 2018; 27 (4), 045019
- Zolfagharian, A., Kaynak, A., Khoo, S.Y., Kouzani, "Pattern-driven 4D printing, *Sens. Actuators, A*, 2018; 274, 231-243
- Derakhshani, M., Berfield, T., Murphy, K.D., "Dynamic Analysis of a Bi-stable Buckled Structure for Vibration Energy Harvester, *Dynamic Behavior of Materials*", Vol. 1. Conference Proceedings of the Society for Experimental Mechanics Series. 2018; 1: 199-208
- Derakhshani, M., Allgeier, B.E., Berfield, T.A., "A MEMS-scale vibration energy harvester based on coupled component structure and bi-stable states", arXiv:1805.04593, 2018
- Hashemi, S. H., Derakhshani, M., and Fadaee, M., *Appl. Math. Modell.*, "An accurate mathematical study on the free vibration of stepped thickness circular/annular Mindlin functionally graded plates", 2013, 37(6), 4147-4164.
- Li, K., Wright, J., Modaresahmadi, S., Som, D., Williams, W., Bird, J.Z., "Designing the first stage of a series connected multistage coaxial magnetic gearbox for a wind turbine demonstrator" *Energy Conversion Congress and Exposition IEEE*, 2017; 1247-1254
- Som, D., Li, K., Kadel, J., Wright, J., Modaresahmadi, S., Bird, J.Z., Williams, W., "Analysis and testing of a coaxial magnetic gearbox with flux concentration halfbach rotors", *IEEE Trans. Magn.*, 2017; 53 (11), 1-6
- Ghasemi, A., Dardel, M., Ghasemi, M.H., "Collective Effect of Fluid's Coriolis Force and Nanoscale's Parameter on Instability Pattern and Vibration Characteristic of Fluid-Conveying Carbon Nanotubes", *J. Pressure Vessel Technol*, 2015; 137 (3), 031301
- Ghasemi, A., Dardel, M., Ghasemi, M.H., "Control of the non-linear static deflection experienced by a fluid-carrying double-walled carbon nanotube using an external distributed load", *Proceedings of the Institution of Mechanical Engineers, Part N: Journal of Nanoengineering and Nanosystems*, 2012; Vol 226, Issue 4, pp. 181 – 190
- Tehrani, M., Ghalamzan, Z., Sarvestani, A., "Polydispersity controls the strength of semi-flexible polymer networks, *Physical biology*", *Phys. Biol.*, 2018; 15 (6), 066002
- Tehrani, M., Moshaei, M.H., Sarvestani, A.S., "Network Polydispersity and Deformation-Induced Damage in Filled Elastomers", 2017; *Macromol. Theory Simul.* 26 (6), 1700038
- Wu, C., Taghvaei, T., Wei, C., Ghasemi, A., Chen, G., Leventis, N., Gao, W., "Multi-scale Progressive Failure Mechanism and Mechanical Properties of Nanofibrous Polyurea Aerogels, *soft matter*", DOI: 10.1039/c8sm01546e, 2018
- Alhavaz, A., Rezaei Dastjerdi M., Ghasemi, A., Ghasemi, A., Alizadeh Sahraei, A., "Effect of untreated zirconium oxide nanofiller on the flexural strength and surface hardness of autopolymerized interim fixed restoration resins". *J Esthet Restor Dent.* 017;29:264-269
- Benedetti, I., Nguyen, H., Soler-Crespo, R.A., Gao, W., Mao, L., Ghasemi, A., Wen, J., Nguyen, S.B., Espinosa, H. D., *J. Mech. Phys. Solids*, 2018;112, 66-88
- Safaei, B., Moradi-Dastjerdi, R., Chu, F., "Effect of thermal gradient load on thermo-elastic vibrational behavior of sandwich plates reinforced by carbon nanotube agglomerations", *Compos. Struct.*, 2018; 192, 28-37
- Hoseinzadeh, S., Sahebi, S.A.R., Ghasemiasl, R. et al. *Eur. Phys. J. Plus* (2017) 132: 197. <https://doi.org/10.1140/epjp/i2017-11455-3>
- R. Ghasemiasl, S. Hoseinzadeh, and M. A. Javadi. *Journal of Thermophysics and Heat Transfer*, Vol. 32, No. 2 (2018), pp. 440-448. <https://doi.org/10.2514/1.T5252>
- S. Hoseinzadeh, R. Ghasemiasl, D. Havaei, A.J. Chamkha, Numerical investigation of rectangular thermal energy storage units with multiple phase change materials, *Journal of Molecular Liquids*, Volume 271, 2018, Pages 655-660,
- Ramezani, A.H., Hantehezadeh, M.R., Ghoranneviss, M. et al. *Appl. Phys. A* (2016) 122: 179.

- Dastan, D., Panahi, S.L. & Chaure, N.B. J Mater Sci: Mater Electron (2016) 27: 12291. <https://doi.org/10.1007/s10854-016-4985-4>
- Dastan, D. Appl. Phys. A (2017) 123: 699. <https://doi.org/10.1007/s00339-017-1309-3>
- Najafi-Ashtiani, H., Bahari, A., Gholipour, S. & Hoseinzadeh, S. Appl. Phys. A (2018) 124: [24.https://doi.org/10.1007/s00339-017-1412-5](https://doi.org/10.1007/s00339-017-1412-5)